Top Catal (2013) 56:950–957
DOI 10.1007/s11244-013-0059-5

ORIGINAL PAPER

Enhanced Sulfur Tolerance of Ceria-Promoted NO_x Storage Reduction (NSR) Catalysts: Sulfur Uptake, Thermal Regeneration and Reduction with H_2(g)

Zafer Say · Evgeny I. Vovk · Valerii I. Bukhtiyarov · Emrah Ozensoy

Published online: 16 May 2013

Abstract SO_x uptake, thermal regeneration and the reduction of SO_x via H_2(g) over ceria-promoted NSR catalysts were investigated. Sulfur poisoning and desulfation pathways of the complex BaO/Pt/CeO_2/Al_2O_3 NSR system was investigated using a systematic approach where the functional sub-components such as Al_2O_3, CeO_2/Al_2O_3, BaO/Al_2O_3, BaO/CeO_2/Al_2O_3, and BaO/Pt/Al_2O_3 were studied in a comparative fashion. Incorporation of ceria significantly increases the S-uptake of Al_2O_3 and BaO/Al_2O_3 under both moderate and extreme S-poisoning conditions. Under moderate S-poisoning conditions, Pt sites seem to be the critical species for SO_x oxidation and SO_x storage, where BaO/Pt/Al_2O_3 and BaO/Pt/CeO_2/Al_2O_3 catalysts reveal a comparable extent of sulfation. After extreme S-poisoning due to the deactivation of most of the Pt sites, ceria domains are the main SO_x storage sites on the BaO/Pt/CeO_2/Al_2O_3 surface. Thus, under these conditions, BaO/Pt/CeO_2/Al_2O_3 surface stores more sulfur than that of BaO/Pt/Al_2O_3. BaO/Pt/CeO_2/Al_2O_3 reveals a significantly improved thermal regeneration behavior in vacuum with respect to the conventional BaO/Pt/Al_2O_3 catalyst. Ceria promotion remarkably enhances the SO_x reduction with H_2(g).

Keywords NSR · NO_x · SO_x · Sulfur poisoning · DeNO_x · Ceria

Z. Say · E. I. Vovk · E. Ozensoy (✉)
Department of Chemistry, Bilkent University, Ankara, Turkey
e-mail: ozensoy@fen.bilkent.edu.tr

E. I. Vovk · V. I. Bukhtiyarov
Boreskov Institute of Catalysis, Novosibirsk, Russia

1 Introduction

Conventional three way catalysts (TWC such as Pt/Rh/CeO_2/Al_2O_3) are known to have a poor nitrogen oxide (NO_x) reduction performance under lean conditions. Thus, lean burn and diesel engines call for an alternative after treatment technology for the elimination of toxic NO_x species. The NO_x storage and reduction (NSR) catalyst technology is a promising candidate for NO_x reduction under lean conditions [1–3]. However, NSR technology suffers from various drawbacks, one of which is associated with the loss of catalytic activity due to the accumulation of sulfur on the NO_x storage sites of the catalyst [4, 5]. As the thermodynamic stability of sulfur oxides (SO_x) on most metal oxide surfaces is typically higher than that of nitrates, sulfur containing species such as sulfates or sulfites can readily block catalytic active sites [6] forming inactive $BaSO_3$, $BaSO_4$, $Al_2(SO_3)_3$ and $Al_2(SO_4)_3$ species [7, 8]. It has been shown in the literature that the sulfur poisoning tolerance of NSR catalysts can be improved by modifying the surface chemistry of the catalysts with the help of additional metal oxide promoters [9]. Ceria has attracted considerable interest as a catalytic promoter and a support material in TWC and NSR applications [10, 11]. Furthermore, ceria is also used as an active component in several important reactions such as water–gas shift (WGS) and steam reforming reactions [12, 13]. Ceria promotion is also known to have a strong influence on the dispersion of precious metals on metal oxide support materials [14]. SO_2 adsorption on γ-Al_2O_3 [15, 16] and CeO_2 surfaces has been extensively studied via FTIR spectroscopy. Waqif et al. [17] investigated a CeO_2–Al_2O_3 mixed-oxide system and demonstrated that this surface had a higher sulfur uptake compared to pure γ-Al_2O_3 or CeO_2 [18]. Previous investigations on the sulfur uptake of Pt/CeO_2 materials have

also shown that Pt incorporation onto the ceria support did not have a significant effect on the nature and amount of adsorbed sulfate species [19]. In contrast to the Pt/CeO_2 system, Yao et al. [20] reported that Pt addition to the pure alumina surface increased the total sulfur uptake. Sulfur storage and the formation of surface SO_x species on conventional NSR systems such as $Pt/BaO/Al_2O_3$ and $Pt/BaCO_3/Al_2O_3$ have also been studied in the literature [21, 22], where it was reported that in addition to sulfites, surface and bulk sulfate species were the major SO_x species formed upon oxidation of SO_2 on these surfaces.

Thus, in this study, we focus on the SO_x uptake, desulfation via thermal regeneration and the reduction of adsorbed SO_x via H_2(g) over ceria-promoted NSR catalysts. In order to obtain an in-depth understanding of the SO_x uptake/release properties of the complex $BaO/Pt/CeO_2/Al_2O_3$ NSR system, a systematic approach is employed. In this approach, SO_x uptake/release and reduction properties of the functional sub-components such as Al_2O_3, CeO_2/Al_2O_3, BaO/Al_2O_3, $BaO/CeO_2/Al_2O_3$, and $BaO/Pt/Al_2O_3$, were studied in a systematic fashion. Through this comprehensive approach, the interplay between different functional components of the ceria-promoted NSR catalysts and its implications on the sulfur tolerance are elucidated.

2 Experimental

2.1 Material Synthesis

All of the materials synthesized in this study were prepared via incipient wetness impregnation method. Binary oxide NO_x storage materials loaded with 20 wt% CeO_2 (i.e. $20CeO_2/Al_2O_3$) or 20 wt% BaO (i.e. $20BaO/Al_2O_3$) were prepared by the impregnation of γ-Al_2O_3 (PURALOX, 200 m^2 g^{-1}, SASOL GmbH, Germany) either with a $Ce(NO_3)_3{\cdot}6H_2O$ (>99.0 %, Fluka, France) or a $Ba(NO_3)_2$ (ACS Reagent, ≥99 %, Riedel-de Häen, Germany) aqueous solution followed by annealing in Ar(g) at 873 K for 2 h.

The $20BaO/20CeO_2/Al_2O_3$ sample containing 20 wt% CeO_2 and 20 wt% BaO was synthesized by the impregnation of γ-Al_2O_3 with a $Ce(NO_3)_3{\cdot}6H_2O$ solution and calcination in air at 823 K for 2 h followed by impregnation with a $Ba(NO_3)_2$ solution (ACS Reagent, ≥99 %, Riedel-de Häen, Germany) and a subsequent annealing in Ar(g) for 2 h at 873 K.

The $20BaO/Pt/Al_2O_3$ sample containing 20 wt% BaO and 1 wt% Pt was synthesized by impregnating γ-Al_2O_3 with a $Pt(NH_3)_2(NO_2)_2$ solution (Aldrich, Diamminedinitritoplatinum(II), 3.4 wt% solution in dilute NH_3(aq)) followed by calcination in air at 823 K for 2 h and successive impregnation with a $Ba(NO_3)_2$ solution and a final annealing in Ar(g) at 873 K.

The $20BaO/Pt/20CeO_2/Al_2O_3$ sample contained BaO, Pt, and CeO_2 loadings of 20, 1, and 20 wt%, respectively. This material was prepared by the impregnation of γ-Al_2O_3 with a $Ce(NO_3)_3{\cdot}6H_2O$ solution and calcination in air at 823 K for 2 h followed by impregnation with a $Pt(NH_3)_2(NO_2)_2$ solution and a subsequent calcination in air at 823 K for 2 h. As the final step, the obtained material was impregnated with a $Ba(NO_3)_2$ solution and annealed in Ar(g) at 873 K for 2 h.

The $20BaO:20CeO_2/Pt/Al_2O_3$ material comprised BaO, Pt, and CeO_2 loadings of 20, 1, and 20 wt%, respectively. For the synthesis of this material, γ-Al_2O_3 was impregnated with a $Pt(NH_3)_2(NO_2)_2$ solution followed by calcination in air at 823 K for 2 h. Next, using a solution containing a dissolved mixture of $Ba(NO_3)_2$ and $Ce(NO_3)_3{\cdot}6H_2O$, co-impregnation was performed. After the co-impregnation, sample was annealed in Ar(g) at 873 K for 2 h.

2.2 Instrumentation

All of the FTIR spectroscopy experiments were conducted in transmission mode using a Bruker Tensor 27 spectrometer coupled to a batch type catalytic reactor whose details are described elsewhere [23]. All of the FTIR spectra were acquired at 323 K. Before FTIR analysis, samples were initially activated in 2 Torr NO_2(g) at 323 K for 5 min followed by annealing at 973 K in vacuum ($<10^{-3}$ Torr) for 5 min. The sulfation of the catalyst samples was carried out by exposing the sample surfaces to a 2.0 Torr (for moderate poisoning experiments) or 10.0 Torr (for extreme poisoning experiments) $SO_2 + O_2$ gas mixture (SO_2:O_2 = 1:10) at 673 K for 30 min. After sulfation, thermal regeneration of the samples was performed by flash-annealing the sulfur-poisoned catalysts to 1,173 K with a heating rate of 12 K min^{-1} under vacuum. For the H_2(g) assisted desulfation and SO_x reduction experiments, 5.0 Torr of H_2(g) was introduced over the sulfated materials at 323 K followed by annealing at 773 K for 30 min in the presence of H_2(g).

NO_2(g) used in the FTIR experiments was synthesized by the reaction of NO (99.9 % purity, Air Products) with O_2 (99.999 % purity, Linde AG) and further purified by subsequent freeze–thaw-pump cycles.

Ex-situ XPS analysis was performed using a SPECS XP spectrometer with a PHOIBOS-100 hemispherical energy analyzer utilizing monochromatic AlKα X-ray irradiation (hv = 1,486.74 eV, 200 W).

3 Results and Discussion

3.1 Qualitative Analysis of the Influence of Ceria on SO_x Oxidation Under Moderate Poisoning Conditions

The effect of ceria promotion on SO_x uptake capacity was investigated via in situ FTIR (Fig. 1). FTIR spectra presented in Fig. 1 were recorded in vacuum after sulfation of each sample with 2.0 Torr of $SO_2 + O_2$ gas mixture (SO_2:O_2 = 1:10) at 673 K for 30 min. These experiments were performed in order to obtain qualitative knowledge regarding the surface SO_x species that are formed on the synthesized catalysts under moderate poisoning conditions. As described in the next section, in order to complement these qualitative FTIR experiments with quantitative S-uptake data, determination of the extent of sulfur poisoning was also studied via XPS. However, due to a relatively lower detection limit of the XPS technique towards SO_x species, quantitative S-uptake measurements were performed under extreme poisoning conditions using 10.0 Torr of $SO_2 + O_2$ gas mixture (see next section for details).

γ-Al_2O_3 and $20CeO_2/Al_2O_3$ materials were initially analyzed as benchmark samples in order to demonstrate the direct effect of ceria domains on alumina in the sulfation process. The SO_x exposure on γ-Al_2O_3 (Fig. 1a, spectrum i) reveals two major vibrational features at 1,374 and 1,098 cm^{-1} corresponding to the asymmetric and symmetric stretching modes of surface sulfates on alumina domains, respectively [24]. A set of minor features below 1,080 cm^{-1} are associated with sulfite species on alumina sites [25, 26]. Furthermore, a minuscule feature can also be observed at 1,168 cm^{-1}, which can be attributed to bulk $Al_2(SO_4)_3$ species [5]. The introduction of SO_x mixture onto $20CeO_2/Al_2O_3$ (Fig. 1a, spectrum ii) leads to the appearance of surface species relatively similar to that of γ-Al_2O_3. The vibrational feature at 1,395 cm^{-1} for $20CeO_2/Al_2O_3$ can be assigned to surface sulfate species on ceria domains [17]. Although the 1,100–1,000 cm^{-1} region of the FTIR spectra for the $20CeO_2/Al_2O_3$ sample is difficult to analyze due to the convoluted nature of the vibrational features, these signals can be attributed to surface sulfite (SO_3^{2-}) species on CeO_2 [18]. The FTIR spectra presented in Fig. 1a clearly point to the fact that ceria promotion of alumina leads to a strong increase in the formation of sulfate and sulfite species upon exposure to $SO_2 + O_2$ mixture at 673 K. This qualitative finding is in very good agreement with the quantitative sulfur uptake measurements performed via XPS that will be discussed in the next section. This observation is also in line with the former investigations, where it was shown that ceria is able to effectively oxidize SO_2 even in the absence of a precious metal center such as Pt [27]. This effect can be attributed to the redox properties of ceria such as its ability to undergo reversible $Ce^{4+} \leftrightarrow Ce^{3+}$ transformations as well as its high oxygen storage and transport capacity.

Figure 1b also reveals the influence of ceria promotion on sulfur uptake of BaO-containing NO_x storage systems. FTIR spectrum of $20BaO/Al_2O_3$ (Fig. 1b, spectrum iii) reveals four different vibrational features at 1,255, 1,167, 1,117 and 1,054 cm^{-1}. While the first couple of vibrational features can be assigned to bulk $BaSO_4$, the latter two signals are associated with surface $BaSO_4$ [5]. Although

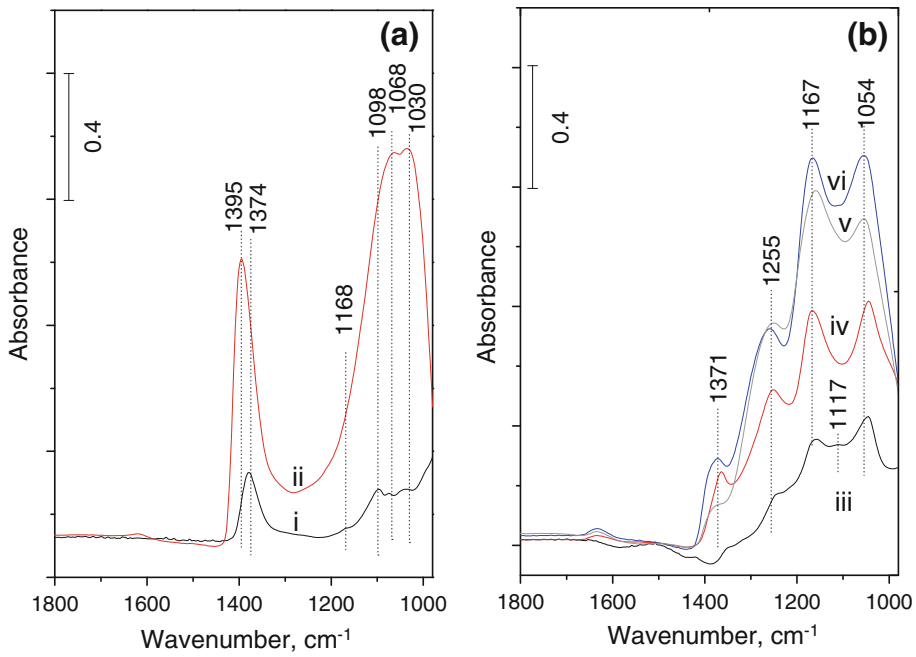

Fig. 1 FTIR spectra acquired after exposing the synthesized catalysts to $SO_2 + O_2$ mixture (P_{total} = 2.0 Torr, SO_2:O_2 = 1:10) at 673 K for 30 min: (*i*) γ-Al_2O_3, (*ii*) $20CeO_2/Al_2O_3$, (*iii*) $20BaO/Al_2O_3$, (*iv*) $20BaO/20CeO_2/Al_2O_3$, (*v*) $20BaO/Pt/20CeO_2/Al_2O_3$, (*vi*) $20BaO/Pt/Al_2O_3$. All spectra were acquired at 323 K in vacuum

the sulfation of the $20BaO/20CeO_2/Al_2O_3$ sample (Fig. 1b, spectrum iv) leads to vibrational features similar to those of the $20BaO/Al_2O_3$ surface, vibrational intensities of all of the adsorbed SO_x species are significantly higher for $20BaO/20CeO_2/Al_2O_3$. Thus, it is apparent that as in the case of pure alumina, ceria promotion of $20BaO/Al_2O_3$ also increases the sulfur uptake. Analysis of the behavior of the Pt-containing NSR catalysts given in Fig. 1b, such as $20BaO/Pt/20CeO_2/Al_2O_3$ (Fig. 1b, spectrum v) and $20BaO/Pt/Al_2O_3$ (Fig. 1b, spectrum vi), suggests that after 2.0 Torr of SO_x mixture exposure at 673 K for 30 min (i.e. under moderate S-poisoning conditions), Pt facilitates SO_x oxidation and increases the sulfur uptake of the catalyst samples. However, under this particular set of sulfation conditions and in the presence of Pt sites, ceria domains do not seem to have a major influence on the total SO_x uptake, emphasizing the critical role of the Pt sites in facilitating SO_2 oxidation and SO_x storage.

In order to demonstrate the significance of Pt sites in SO_2 oxidation and SO_x storage processes, we designed a control experiment where we synthesized a $20BaO:20CeO_2/Pt/Al_2O_3$ catalyst by co-impregnation of $Ba(NO_3)_2$ and $Ce(NO_3)_3{\cdot}6H_2O$ onto Pt/Al_2O_3. On the $20BaO:20CeO_2/Pt/Al_2O_3$ catalyst surface, Pt sites are expected to be partially covered with ceria and baria domains, thereby decreasing the number of available (i.e. exposed) Pt sites that can take part in SO_x oxidation with respect to that of the $20BaO/Pt/20CeO_2/Al_2O_3$ surface. Fig. 2 shows the FTIR spectra obtained after exposing $20BaO/Pt/20CeO_2/Al_2O_3$ (Fig. 2, spectrum i) and $20BaO:20CeO_2/Pt/Al_2O_3$ (Fig. 2, spectrum ii) surfaces to $SO_2 + O_2$ mixture at 673 K (2.0 Torr, $SO_2:O_2 = 1:10$) for 30 min. Fig. 2 clearly indicates that all of the vibrational features within 1,350–1,000 cm^{-1} are markedly suppressed for the co-impregnation sample. This observation is in harmony with the presumably smaller number of available exposed Pt sites on the $20BaO:20CeO_2/Pt/Al_2O_3$ surface that can take part in the SO_2 oxidation and SO_x storage. The stronger 1,383 cm^{-1} signal associated with surface sulfates on ceria domains for the $20BaO:20CeO_2/Pt/Al_2O_3$ sample is also consistent with the presence of a greater extent of available ceria domains on the co-impregnation sample, as opposed to the weaker corresponding signal for $20BaO/Pt/20CeO_2/Al_2O_3$, where a larger portion of the ceria domains are covered by BaO sites due the sequential impregnation method used in the synthesis of the latter catalyst. Thus, it can be argued that under moderate S-poisoning conditions, SO_2 oxidation occurs more efficiently on the precious metal (Pt) sites than the neighboring BaO, CeO_2 or Al_2O_3 domains and the generated sulfite and sulfate species spill over from the precious metal center onto the oxide domains where they are stored in an effective manner.

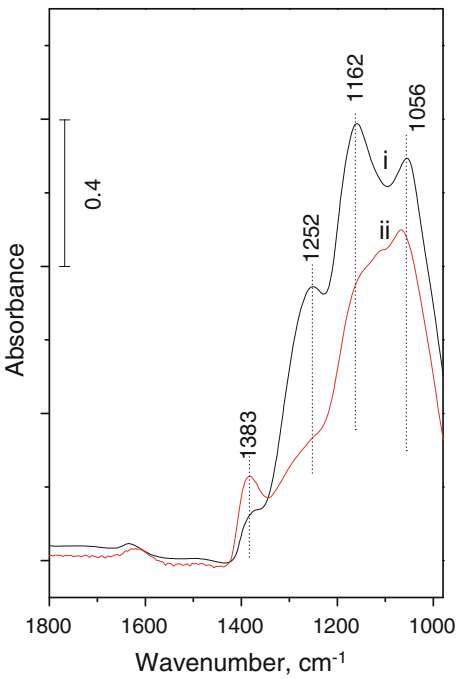

Fig. 2 FTIR spectra acquired after SO_x (2.0 Torr, $SO_2:O_2 = 1:10$) exposure at 323 K followed by annealing at 673 K in the gas mixture for 30 min: (*i*) $20BaO/Pt/20CeO_2/Al_2O_3$, (*ii*) $20BaO:20CeO_2/Pt/Al_2O_3$. All spectra were acquired at 323 K in vacuum

3.2 Quantitative Analysis of the Influence of Ceria on the Total Sulfur Uptake under Extreme Poisoning Conditions

Ex-situ XPS analysis was performed in order to gain a quantitative understanding of the SO_x uptake behavior of the synthesized materials. Prior to the XPS measurements, each sample was exposed to extreme poisoning conditions, which included exposure to 10 Torr $SO_2 + O_2$ gas mixture ($SO_2:O_2 = 1:10$) at 673 K for 30 min. As mentioned above, although these extreme sulfur poisoning conditions were chosen due to a relatively low sensitivity of the XPS technique towards S, these conditions also enabled us to investigate the extensive sulfation of the synthesized materials and compare these findings with the moderate S-poisoning conditions analyzed via FTIR. XPS data revealed that for all samples, S2p region of the corresponding XP spectra typically included a major feature located at a BE of ~168.5 eV which was associated with S^{6+} state (i.e. sulfates). Figure 3 presents the relative surface concentration of S atoms (in percent) on the investigated surfaces after extensive S-poisoning with respect to all atoms on the surface (i.e. S, Al, O, Ba, Ce, Pt). Quantitative total S-uptake trends measured via XPS upon extensive S-poisoning (Fig. 3) are generally similar to the qualitative findings obtained from the current FTIR measurements (Fig. 1). Total S-uptake of the investigated

samples after extensive S-poisoning can be ranked as follows: γ-Al_2O_3 < 20BaO/Al_2O_3 < 20CeO_2/Al_2O_3 < 20BaO/20CeO_2/Al_2O_3 < 20BaO/Pt/Al_2O_3 < 20BaO/Pt/20CeO_2/Al_2O_3. Figure 3 indicates that ceria incorporation onto the γ-Al_2O_3 and 20BaO/Al_2O_3 surfaces significantly increases the total S-uptake, which is in very good agreement with the FTIR results. The higher S surface atomic concentration on poisoned 20CeO_2/Al_2O_3 surface compared to that of poisoned 20BaO/Al_2O_3 can be explained by the difference in the dispersion of ceria and BaO domains on the alumina surface. Our XPS measurements (data not shown) indicate that Ce surface atomic concentration on 20CeO_2/Al_2O_3 is ~17 %, while Ba surface atomic concentration on 20BaO/Al_2O_3 is ~2 %. In other words, unlike BaO, ceria is dispersed much better on the alumina surface and the relatively higher S atomic concentrations on the poisoned 20CeO_2/Al_2O_3 surface are associated with the high ceria dispersion. Our XPS results also reveal that BaO loading on ceria-promoted materials significantly suppresses the Ce XPS signal (roughly by a factor of 15). This finding clearly suggests that BaO preferably covers ceria domains, and ceria domains function as anchoring sites for BaO.

Figure 3 also illustrates that addition of Pt centers to 20BaO/Al_2O_3 and 20BaO/20CeO_2/Al_2O_3 drastically facilitates the total S-uptake of the NSR catalysts, suggesting that Pt centers are the crucial sites for SO_2 oxidation. A noticeable discrepancy between the sulfation trends under moderate (Fig. 1) and extensive (Fig. 3) poisoning conditions can be realized for the 20BaO/Pt/Al_2O_3 and 20BaO/Pt/20CeO_2/Al_2O_3 samples. Although both of these samples show comparable extent of sulfation under moderate poisoning conditions, ceria containing sample (i.e. 20BaO/Pt/20CeO_2/Al_2O_3) reveals a significantly higher total S-uptake under extreme poisoning conditions. It is likely

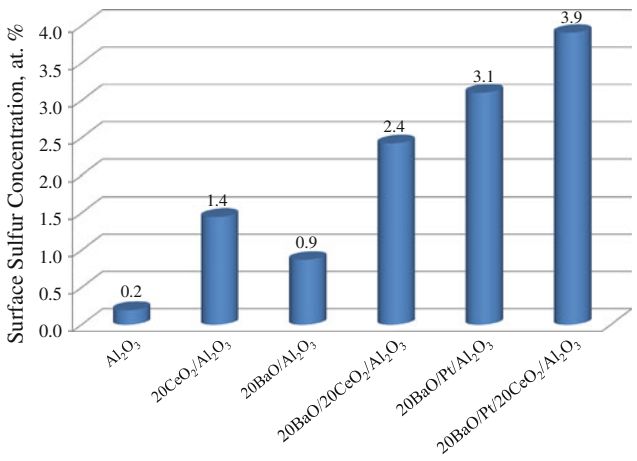

Fig. 3 Quantitative determination of the concentration of S atoms on the synthesized catalyst surfaces via XPS after extensive S-poisoning (10 Torr, 673 K, SO_2:O_2 = 1:10)

that under moderately poisoning conditions, Pt sites are not completely deactivated and are able to sustain their functionality in SO_2 oxidation and facilitate the spill over of SO_x species on BaO, CeO_2, and Al_2O_3 domains. On the other hand, under extreme poisoning conditions, presumably a large fraction of the Pt sites are deactivated by SO_x, limiting the SO_x spill over particularly on the 20BaO/Pt/Al_2O_3 sample. However, even at this later stage of S-poisoning, ceria promoted the 20BaO/Pt/20CeO_2/Al_2O_3 sample seems to be capable of storing SO_x species, most likely due to SO_2 oxidation directly on ceria domains with the help of the oxygen storage and transport properties of ceria.

3.3 Effect of S-Poisoning on NO_x Storage Capacity over Ce-Free and Ce-Promoted NSR Catalysts

Suppression of the NO_x storage capacity (NSC) of the NSR catalysts due to sulfur poisoning is a vital issue directly affecting the operational lifetime of the catalysts. Since both NO_x(g) and SO_x(g) have the acidic character, they compete for similar basic adsorption sites on the NSR catalyst surface. This behavior can also be readily noticed in Figs. 1 and 3, where incorporation of more basic domains onto the γ-Al_2O_3 surface such as BaO or CeO_2 radically increases the S-uptake. As sulfite and sulfate species typically bind to the BaO, CeO_2, and Al_2O_3 domains stronger than nitrates and nitrites, SO_x species can also effectively block active sites for NO_x storage [6, 7]. This can be clearly demonstrated by in situ FTIR measurements. Figure 4 shows such experiments, in which NO_x adsorption characteristics of fresh (Fig. 4, black spectra) and S-poisoned (Fig. 4, red spectra) γ-Al_2O_3, 20CeO_2/Al_2O_3, 20BaO/Pt/Al_2O_3, and 20BaO/Pt/20CeO_2/Al_2O_3 samples were investigated in a comparative fashion under moderate poisoning conditions (2.0 Torr SO_2 + O_2 gas mixture, SO_2:O_2 = 1:10 at 673 K, 30 min). Figure 4 shows that NO_2 adsorption (5.0 Torr NO_2(g), 323 K, 10 min) on the investigated samples reveals typical vibrational features within 1,700–1,000 cm^{-1} corresponding to various nitrate and nitrite species. A detailed analysis and assignments for the NO_x vibrational features can be made by referring to the previous studies in the literature [28–33] as well as our recently published reports [9, 23, 30, 34, 35]. Since the main emphasis of the current work is the sulfur surface chemistry, here we will mainly focus on the qualitative trends associated with the relative suppression of NSC due to sulfur poisoning.

Figure 4a suggests that in addition to regular nitrite/nitrate vibrational features, S-poisoned γ-Al_2O_3 (Fig. 4, spectrum ii) and 20CeO_2/Al_2O_3 samples (Fig. 4, spectrum iv) also reveal surface sulfate (1,384 cm^{-1}) and sulfite (1,100–1,000 cm^{-1}) species. Although the extent of NSC suppression due to S-poisoning on γ-Al_2O_3 is rather minor,

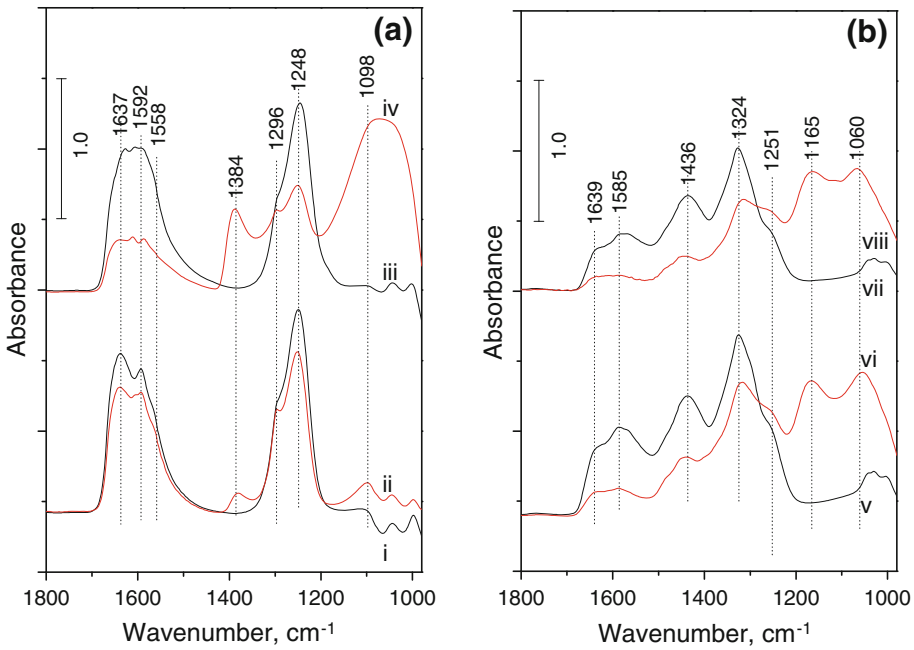

Fig. 4 FTIR spectra acquired after NO_2 saturation (5.0 Torr NO_2(g), 323 K, 10 min) of fresh (black spectra) and S-poisoned surfaces (red spectra) at 2.0 Torr, 673 K, SO_2:O_2 = 1:10: (*i,ii*) γ-Al_2O_3, (*iii, iv*) 20CeO_2/Al_2O_3, (*v, vi*) 20BaO/Pt/Al_2O_3, and (*vii, viii*) 20BaO/Pt/20CeO_2/Al_2O_3. All spectra were acquired at 323 K in vacuum

it is much more significant on 20CeO_2/Al_2O_3. Clearly, there is a direct correlation between the relative S-uptake trends presented in Figs. 1, 2, and 3 and the extent of NSC suppression (Fig. 4). These observations support the fact that NO_x(g) and SO_x(g) species compete for similar adsorption sites on NSR catalysts.

As shown in Fig. 4b (spectra v-viii), analogous sets of experiments were also performed for Pt-containing catalysts (i.e. 20BaO/Pt/Al_2O_3 and 20BaO/Pt/20CeO_2/Al_2O_3). Vibrational features associated with NO_x species for these surfaces appear at 1,639 cm^{-1} (due to surface nitrates on γ-Al_2O_3 and/or CeO_2), 1,585 and 1,324 cm^{-1} (due to surface nitrates on BaO), and 1,436 cm^{-1} (due to bulk nitrates on BaO). Extent of NSC suppression of both of these samples under moderately poisoning conditions is very similar, which is in perfect agreement with Fig. 1, suggesting that both of these surfaces have similar SO_x species with comparable surface SO_x coverages.

3.4 Influence of Ceria on the Direct Thermal Regeneration Performance of NSR Catalysts in Vacuum

In order to investigate the effect of ceria promotion on the thermal regeneration performance of S-poisoned materials in vacuum, we have initially poisoned 20BaO/Pt/Al_2O_3 and 20BaO/Pt/20CeO_2/Al_2O_3 catalysts under moderate poisoning conditions (2.0 Torr $SO_2 + O_2$ gas mixture, SO_2:O_2 = 1:10 at 673 K, 30 min) and then flash-annealed these samples to 1,173 K in vacuum. Figure 5 shows the FTIR spectra obtained after this poisoning and thermal regeneration treatment of the 20BaO/Pt/Al_2O_3 (Fig. 5, spectrum i) and 20BaO/Pt/20CeO_2/Al_2O_3 (Fig. 5, spectrum ii) catalysts. Comparison of the relative spectra in Figs. 1 and 5 clearly indicates that the remaining amount of SO_x species on the catalyst surfaces after thermal regeneration is significantly smaller than the original amount of SO_x species present on the poisoned catalysts (note the difference between the IR absorbance intensity scales in Figs. 1, 5).

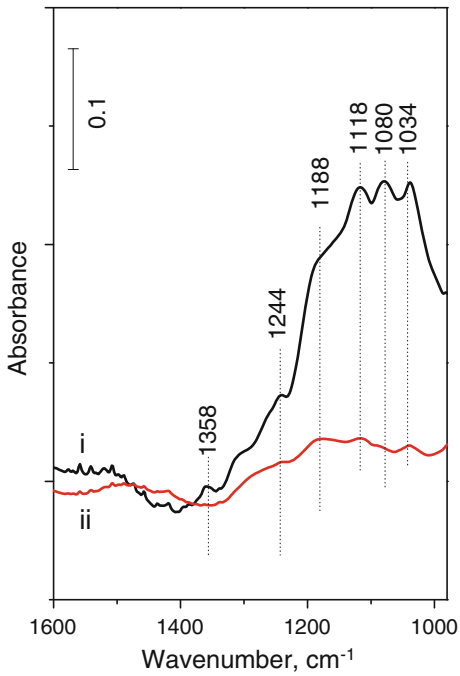

Fig. 5 FTIR spectra acquired after annealing S-poisoned (2.0 Torr, 673 K, 30 min, SO_2:O_2 = 1:10): (*i*) 20BaO/Pt/Al_2O_3 and (*ii*) 20BaO/Pt/20CeO_2/Al_2O_3 surfaces at 1,173 K in vacuum. All spectra were acquired at 323 K in vacuum

Furthermore, it is apparent in Fig. 5 that the ceria promoted NSR catalyst (i.e. 20BaO/Pt/20CeO_2/Al_2O_3) has a significantly superior thermal regeneration capability with respect to ceria-free NSR catalyst. Thus, it is apparent that ceria promotion of NSR catalysts noticeably improves the sulfur removal via direct thermal regeneration. One of the possible explanations for this observation could be the lower thermodynamic stability of the adsorbed SO_x species on ceria domains or Pt/CeO_2, BaO/CeO_2 or Al_2O_3/CeO_2 interfaces. Alternatively, it is also plausible that ceria sites are partially reduced during vacuum annealing and the generated oxygen-deficient defect sites on the ceria domains reduce the sulfate and sulfite species to relatively weakly adsorbed SO_2 species which can readily desorb from the surface at elevated temperatures.

3.5 Enhancement of SO_x Reduction with H_2(g) via Ceria Promotion of NSR Catalysts

Removal of SO_x species on S-poisoned NSR catalysts via reduction with H_2(g) was also investigated with in situ FTIR spectroscopy over conventional (20BaO/Pt/Al_2O_3) and ceria-promoted NSR catalysts (20BaO/Pt/20CeO_2/Al_2O_3). Spectra i and iii in Fig. 6 were acquired after 2.0 Torr $SO_2 + O_2$ (SO_2:O_2 = 1:10 at 673 K, 30 min) adsorption on fresh catalyst surfaces, respectively. These spectra are in perfect agreement with the corresponding spectra shown in Fig. 1. On the other hand, spectra ii and iv correspond to the FTIR spectra obtained after treating the S-poisoned 20BaO/Pt/Al_2O_3 and 20BaO/Pt/20CeO_2/Al_2O_3 catalysts with 5.0 Torr of H_2(g) at 773 K for 30 min, respectively. Figure 6 clearly shows that reduction of SO_x species occurs to a limited extent on the conventional NSR catalyst in which sulfate species are predominantly reduced to sulfites, while SO_x vibrational features almost completely disappear on the ceria-promoted NSR catalyst. This experiment evidently demonstrates the strong influence of ceria promotion on the enhancement of the SO_x reduction with H_2(g) on S-poisoned NSR catalysts. It is worth mentioning that these observations are in line with one of our recent studies on NO_x reduction on ceria-promoted NSR catalysts with H_2(g) [34], where we have observed that ceria incorporation to the conventional 20BaO/Pt/Al_2O_3 NSR catalyst significantly facilitated the reduction of NO_x species to N_2O(g) and N_2(g). In this recent study [34], it was suggested that the enhanced NO_x reduction with H_2(g) on the 20BaO/Pt/20CeO_2/Al_2O_3 catalyst can be associated with the reduction of the ceria domains and the formation of oxygen defect centers which can directly take part in the reduction of NO_x species and/or assist H_2(ad) activation. Furthermore, it was also demonstrated by Raman spectroscopy and in situ FTIR spectroscopy that the presence of unique Pt–O–Ce sites at the Pt/CeO_2 interface can also aid the NO_x reduction with H_2(g) [34, 36]. Thus, it is possible that similar factors may also play an important role in the SO_x reduction with H_2(g) on the 20BaO/Pt/20CeO_2/Al_2O_3 catalyst.

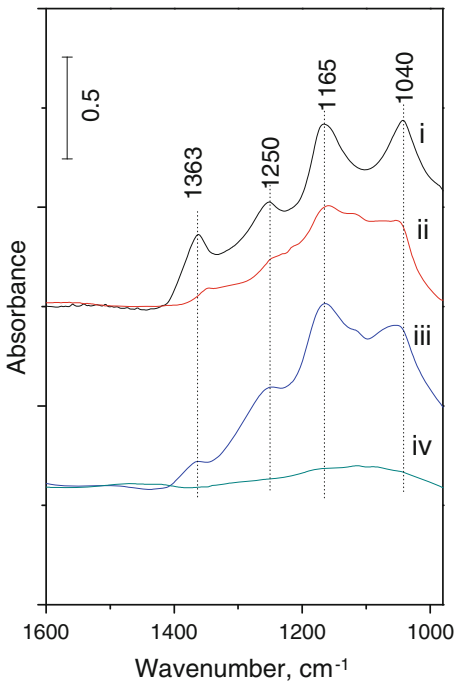

Fig. 6 FTIR spectra acquired after sulfation (2.0 Torr, 673 K, 30 min, SO_2:O_2 = 1:10) followed by reduction with H_2(g) (5.0 Torr, 773 K, 30 min): (*i, ii*) 20BaO/Pt/Al_2O_3 and (*iii, iv*) 20BaO/Pt/20CeO_2/Al_2O_3 (see text for details). All spectra were acquired at 323 K in vacuum

4 Conclusions

In the current report, we investigated the SO_x uptake, thermal regeneration and the reduction of adsorbed SO_x via H_2(g) over ceria-promoted NSR catalysts. In order to elucidate the sulfur poisoning and desulfation pathways of the complex BaO/Pt/CeO_2/Al_2O_3 NSR system, a systematic approach was employed where the functional sub-components such as Al_2O_3, CeO_2/Al_2O_3, BaO/Al_2O_3, BaO/CeO_2/Al_2O_3, and BaO/Pt/Al_2O_3 were studied in a systematic fashion. Our findings can be summarized as follows:

- Incorporation of ceria significantly increases the S-uptake of Al_2O_3 and BaO/Al_2O_3 under both moderate and extreme S-poisoning conditions.
- Under moderate S-poisoning conditions, Pt sites seem to be the critical species for SO_x oxidation, where BaO/Pt/Al_2O_3 and BaO/Pt/CeO_2/Al_2O_3 catalysts reveal a comparable extent of sulfation.

- After extreme S-poisoning, upon deactivation of most of the Pt sites, ceria promoted NSR catalyst (i.e. BaO/Pt/CeO_2/Al_2O_3) stores more sulfur than the conventional BaO/Pt/Al_2O_3 catalyst.
- Suppression of the NO_x storage capacity (NSC) of S-poisoned NSR catalysts monotonically increases with increasing the total S-uptake.
- Ceria-promoted NSR catalyst (i.e. BaO/Pt/CeO_2/Al_2O_3) reveals a notably improved thermal regeneration behavior in vacuum with respect to the conventional BaO/Pt/Al_2O_3 catalyst.
- Ceria promotion remarkably enhances the SO_x reduction with H_2(g).
- Improvement of the desulfation behavior of the ceria promoted NSR catalysts is likely to be associated with the presence of oxygen deficient defect sites on ceria and the reactive Pt–O–Ce sites at the Pt/CeO_2 interface.

Acknowledgments E.O. acknowledges support from Turkish Academy of Sciences (TUBA) through the "Outstanding Young Investigator" Grant. E.V. and V.B. acknowledge RFBR (Russia), Grant #12-03-91373-CT_a, for financial support.

References

1. Kato K, Nohira H, Nakanishi K, Iguchi S, Kihara T, Muraki H (1993) Eur Patent 0,573,672 A1
2. Myioshi N, Matsumoto S, Katoh K, Tanaka T, Harada K, Takahashi N, Yokota K, Sugiura M, Kasahara K (1995) SAE Technical Papers Series 950809
3. Fridell E, Skogludh M, Westerberg B, Johansson S, Smedler G (1999) J Catal 183:196
4. Eppling WS, Campbell LE, Yezerets A, Currier NW, Parks JE II (2004) Catal Rev 46:163
5. Sedlmair CH, Seshan K, Jentys A, Lercher JA (2002) Catal Today 75:413
6. Gill LJ, Blakeman PG, Twigg MV, Walker AP (2004) Top Catal 28:1
7. Matsumoto S, Ikeda Y, Suzuki H, Ogai M, Miyoshi N (2000) Appl Catal B 25:115
8. Mahzoul H, Limousy L, Brilhac JF, Gilot P (2000) J Anal Appl Pyrolysis 56:179
9. Sentürk GS, Vovk EI, Zaikovskii VI, Say Z, Soylu AM, Bukhtiyarov VI, Ozensoy E (2012) Catal Today 184:54
10. Rohr F, Peter SD, Lox E, Kogel M, Sassi A, Juste L, Rigaudeau C, Belot G, Gelin P, Primet M (2005) Appl Catal B 56:201
11. Casapu M, Grunwaldt J, Maciejewski M, Wittrock M, Gobel U, Baiker A (2006) Appl Catal B 63:232
12. Hilaire S, Wang X, Luo T, Gorte RJ, Wagner J (2001) Appl Catal A 215:271
13. Panagiotopoulou P, Kondarides DI (2006) Catal Today 112:49
14. Nagai Y, Hirabayashi T, Dohmae K, Takagi N, Minami T, Shinjoh H, Matsumoto SI (2006) J Catal 242:103
15. Saur O, Bensitel M, Mohammed Saad AB, Lavalley JC, Tripp CP, Morrow BA (1986) J Catal 99:104
16. Chang C (1978) J Catal 53:374
17. Waqif M, Bazin P, Saur O, Lavalley JC, Blanchard G, Touret O (1997) Appl Catal B 11:193
18. Waqif M, Pieplu A, Saur O, Lavalley JC, Blanchard G (1997) Solid State Ionics 95:163
19. Bazin P, Saur O, Lavalley JC, Blanchard G, Visciglio V, Touret O (1997) Appl Catal B 13:265
20. Yao H, Stepien H, Gandhi H (1981) J Catal 67:231
21. Abdulhamid H, Fridell E, Dawody J, Skoglundh M (2006) J Catal 241:200
22. Su Y, Amiridis D (2004) Catal Today 96:31
23. Kayhan E, Andonova SM, Sentürk GS, Chusuei CC, Ozensoy E (2010) J Phys Chem C 114:357
24. Chang CC (1978) J Catal 53:374
25. Yao HC, Stepien HK, Gandhi HS (1981) J Catal 67:231
26. Datta A, Cavel RG, Tower RW, George ZM (1985) J Phys Chem 89:443
27. Bazin P, Saur O, Lavalley JC, Le Govic AM, Blanchard G (1998) Stud Surf Sci Catal 116:571
28. Westerberg B, Fridell E (2001) J Mol Catal A 165:249
29. Sedlmair CH, Seshan K, Jentys A, Lercher JA (2003) J Catal 214:308
30. Ozensoy E, Herling D, Szanyi J (2008) Catal Today 136:46
31. Szanyi J, Kwak JH, Chimentao RJ, Peden CHF (2007) J Phys Chem C 111:2661
32. Szailer T, Kwak JH, Kim DH, Hanson JC, Peden CHF, Szanyi J (2006) J Catal 239:51
33. Szanyi J, Kwak JH, Kim DH, Wang X, Chimentao RJ, Hanson J, Epling WS, Peden CHF (2007) J Phys Chem C 111:4678
34. Say Z, Vovk EI, Bukhtiyarov VI, Ozensoy E (2013) Appl Catal B. doi:10.1016/j.apcatb.2013.04.075
35. Andonova SM, Sentürk GS, Ozensoy E (2010) J Phys Chem C 114:17003
36. Lin W, Herzing AA, Kiely CJ, Wachs IE (2008) J Phys Chem C 112:5942